Unizik Journal of Technology, Production and Mechanical Systems (UJTPMS)

journal homepage: https://journals.unizik.edu.ng/index.php/ujtpms/about
PRINT ISSN: 1115-7143 || ONLINE ISSN: 1115-7453

Production of Ceiling Board from Agricultural Wastes Products (Breadfruit Seed Coats and Rice Husk) using Epoxy Resin as Binder

Emmanuel Chinagorom Nwadike[1*], Echezona Nnaemeka Obika [1]

[1]Department of Mechanical Engineering, Nnamdi Azikiwe University, Awka, PMB 5025, Nigeria

ARTICLE INFO

Article history:
Received Feb 7, 2024
Revised Apr 25, 2024
Accepted Jun 9, 2024

Available online Jun 13, 2024

Keywords:
Composite, Sustainable reinforcements, Epoxy resin, Rice husk, Breadfruit seed

ABSTRACT

This study focused on the sustainable utilization of Breadfruit Seed (BFS) and Rice Husk (RHK) fibres as reinforcements for Epoxy Resin (EPR) matrices. The methodology encompassed the collection and preparation of RHK and BFS, culminating in the production of composite ceiling boards. Through a process involving washing, drying, and chemical treatment, impurities were extracted and binding properties with epoxy resin were enhanced. The fabrication of mild steel molds and spacers ensured precision in casting, while careful consideration was given to the resin-to-hardener ratio in EPR preparation. Emphasis was placed on achieving uniformity and structural integrity in the composite materials during production. Analysis of composite densities revealed a narrow range (5.81-7.04 g/cm^3), highlighting their lightweight characteristics. Water absorption tests revealed varying capacities influenced by composition, with lower epoxy resin content compositions exhibiting higher absorption rates. Additionally, thickness swelling results showed the significant impact of composition variations on dimensional stability, highlighting the necessity for thorough material formulation. Moreover, employing the optimization tool yielded an optimal composition of 14.667 g of RHK, 38.665 g of BFS, and 12.653 g of EPR, resulting in a ceiling board with a density of 6.001 g/cm^3, thickness swell of 9.81%, and water absorption of 4.016%. This study illuminates the potential of BFS and RHK as sustainable reinforcements for EPR matrices, providing valuable insights for the advancement of eco-friendly composite materials.

1. Introduction

The concept of "waste" typically evokes thoughts of undesirable and obsolete items that have exceeded their utility, necessitating immediate disposal, often without due consideration for the environmental consequences. In Nigeria, a nation rich in agricultural produce, an excess of ten million tons of agricultural waste is generated annually. This encompasses a diverse array of materials such as wheat straw, fruit bunches, hazelnut shells and husks, peanut shells, coffee husks, rice straw, maize husks, rice husks, and breadfruit seed coatings. Surprisingly, some of these ostensibly valueless waste products can be repurposed through various processes into new, environmentally friendly products that not only address waste management concerns but also contribute to the economic development of society. Considering rice husks, the natural fibrous sheaths that encapsulate rice grains as they mature in the paddy fields. Despite their abundance, these husks are frequently overlooked and discarded as waste material following the rice milling process. However, their inherent properties and sustainable availability present an opportunity for innovative utilization in various applications, such as eco-friendly construction materials, agricultural amendments, and renewable energy sources. In many rice-producing countries, a substantial portion of husks is either incinerated or dumped as waste [1]. Local agro waste materials, such as rice husks, have been explored for their potential in creating construction materials, including particle boards, thermal insulators, masonry composites/bricks, cementitious binders, and aggregates [2].

*Corresponding author: ec.nwadike@unizik.edu.ng

In South Eastern Nigeria, common agricultural waste like breadfruit seed coatings and rice husks is frequently disposed of through incineration or careless burning, with detrimental effects on the environment. Poor disposal practices of these agricultural wastes contribute to environmental pollution, primarily through indiscriminate dumping (leading to land, water, and air pollution) and burning (contributing to the greenhouse effect). However, some of these waste products can be repurposed into environmentally friendly alternatives, adding value to Nigeria's economic development. Despite the considerable attention given to recycling "post-consumer" waste materials like glass bottles, aluminum cans, plastic jugs, and old newspapers, agricultural waste recycling, particularly breadfruit seed coatings and rice husks, has received relatively little attention until recently. Some notable works focus on producing ceiling boards using various agro waste materials, including jatropha curcas seedcake material [3], watermelon peels [4], bamboo [5], corn cobs and cassava stalks [6], rice husk [7,8,9], banana fibers [10], and breadfruit seed coats [11]. An environmentally friendly alternative for these agricultural wastes lies in their utilization for manufacturing particulate composites or ceiling boards. These boards typically consist of particles bound together with synthetic adhesives or other binders, which are then pressed under heat until the adhesives cure. This approach not only addresses the issue of agricultural waste but also presents an eco-friendly solution for the construction and building material industry. The discourse on waste management is evolving to encompass a broader range of materials, including agricultural waste. The potential of recycling agricultural waste into valuable products, such as particulate composites or ceiling boards, is gaining recognition. This not only offers an environmentally friendly alternative to conventional disposal practices but also contributes to economic development.

2. Materials and Methods

2.1 Collection and Preparation of Rice Husk and Bread fruit Seed Coating

The rice husks sourced from the rice mill in Achalla and the breadfruit seed coats obtained from the dumpsite at Eke Awka Market were subsequently transported to the Chemical Laboratory at Nnamdi Azikiwe University in Awka, Anambra State. It was in this laboratory setting that the research was done.

2.2 Preparation of Rice Husk and Breadfruit seed coating

Following the collection phase, both the rice husk (RHK) and breadfruit seed (BFS) coating underwent meticulous processing. They were initially washed in separate containers with water to eliminate impurities like dust, small rice particles, and fine sand particles. Subsequently, the materials were subjected to a drying process in an oven at a temperature of 70°C for 12 hours, effectively eliminating any residual moisture. Upon completion of the drying process, 1 kg of each material; RHK and BFS, was accurately measured using a digital weighing scale. The materials were then individually immersed in a 1 mol/dm^3 solution of NaOH for one hour. This step served the dual purpose of removing pigments from the breadfruit coat and extracting cellulose, hemicelluloses, and lignin from the rice husks. The targeted removal of cellulose, hemicelluloses, and lignin aimed to enhance the binding properties of both the husks and coats with the resin. Post the NaOH treatment, the RHK and BFS underwent neutralization using a 0.5 mol/dm^3 solution of acetic acid. Following the neutralization process, the RHK and BFS underwent thorough washing with water to eliminate any residual acetic acid. Subsequently, the materials were subjected to oven drying at a temperature of 105°C for a duration of 24 hours. The dried materials were then meticulously ground and sieved to a particle size of 600 micrometers using B.S sieves. This sieving process aimed to eliminate oversized and undersized particles, ensuring homogeneity in the final composition. The goal was to facilitate optimal adhesion of epoxy resins, binding the RHK and BFS seamlessly. This meticulous approach was designed to enhance the overall uniformity of the composite material, thereby improving its structural integrity and performance.

2.3 Preparation of mold and spacer for making sample Ceiling board

Mild steel sheets were precisely cut and skillfully formed into various sizes to function as molds for the test samples. These molds were accurately crafted to adhere to specific dimensions, measuring 250mm by 250mm, with allowances made for subsequent machining processes. For the creation of spacers, pieces of mild steel bars were cut to the required lengths and expertly welded to form a square shape. The dimensions of the spacer, including its length, breadth, and thickness, were precisely maintained at 60mm × 60mm × 7mm (Fig. 1.0). The fabrication process involved cutting four pieces of mild steel bars to the specified length of 60mm from the original mild steel sheet. These bars were then adeptly welded to create a square shape, followed by a meticulous polishing step to achieve a refined surface finish. This careful construction of molds and spacers ensures the accuracy and integrity of the subsequent test samples, contributing to the precision and reliability of the experimental setup.

Figure 1: Fabricated mold and spacer

2.4 Preparation of Epoxy Resins

The epoxy resin utilized in the experiment comprises two distinct components: a resin of grade 3554A and a hardener of grade 3554B. The combination of these two components initiates a chemical reaction, causing them to transition from a liquid state to a solid form. Precise measurement and thorough mixing are imperative to ensure the proper curing of the epoxy resin. In this study, the Epoxy resin was carefully prepared in a specific ratio, adhering to a formulation of 3 parts resin to 1 part hardener (3:1). Accurate volumes of the resin and hardener were measured and subsequently combined in a container. The mixture was then stirred at a low speed for a duration of 10 minutes until a uniform consistency, tackiness, and an exothermic reaction were achieved. The resultant mixture, characterized by its uniformity and the occurrence of an exothermic reaction, was deemed suitable for the production process. This methodical approach to resin preparation ensures the optimal chemical reactions required for the subsequent stages of production.

2.5 Production of the Ceiling board

In the production of ceiling boards, the finely ground rice husk and breadfruit coat were carefully weighed using a scale, and they were grouped based on their specific weight compositions required for each sample. The adhesive, proportional to its designated percentage concerning the batched particles, was accurately weighed. The measured volume of adhesive, in the form of epoxy resin, was then poured into a pan. Approximately half of the batched or measured loose particles were subsequently added to the pan containing the adhesive. Thorough mixing of the particles with the adhesive was performed using a spatula. Following this initial mixing, the remaining batch of particles was introduced into the mixture. The entire composition was stirred thoroughly until the adhesive was uniformly distributed, resulting in a homogeneous mixture. This process was repeated for other batched compositions of rice husk/breadfruit coat/adhesives to produce additional replicates. By adhering to this systematic procedure, the production ensured consistent and controlled mixing, contributing to the uniformity and quality of each ceiling board replicate. The approach aimed to achieve reproducibility and reliability in the manufacturing process.

2.6 Casting and Pressing Operation

The homogeneous mixture obtained during the mixing process was carefully transferred into the mold, filling it to a thickness of 10mm, which is 1.5 times the intended 7mm panel thickness. Prior to filling the mold, both the mold and spacer were greased with oil to facilitate the easy removal of the sample after pressing. A metal spatula, acting as a tamping rod, was employed to tamp the composite. This step served to eliminate air voids, level the surface, and create a compacted surface. Once tamped, the mold cover was placed, and the mold was introduced into a manual pressure press machine (Fig. 2.0) for compression. A metal slab was positioned on top before compressing to reduce the mold thickness to the desired 7mm at room temperature. The pressure was maintained at 150 bar at 150^{o}C for 15 minutes. Subsequently, the mold was removed and allowed to cool for 10 minutes before the compacting pressure (the cover) was removed. The resulting composite sample was then left to cool further for several minutes. In total, 10 samples were cast following which they were cut into smaller pieces for various tests. This continuous process ensures the consistency and precision required for the subsequent analyses and assessments of the produced composite samples.

Figure 2 Mold in the Pressure press

2.7 Optimization of particle board Production

The production of the fibre-board was optimized using central composite design via response surface methodology (RSM). The factors considered for the optimization were quantity (g) of rice husk, breadfruit coat (g) and epoxy (g). The response of interest were % water absorption, % thickness swell and density Kg/cm^{3}. Design Expert Version.10.0.1 software was used to optimize the synthesis process. The constraints variables used for the design and the CCD matrix is shown in Table 1.

Table 1: Constraint variables and the ranges

Name	Goal	Lower Limit	Upper Limit	Lower Weight	Upper Weight	Importance
A:Rice Husk	is in range	0	60	1	1	3
B:BFC	is in range	0	60	1	1	3
C:Epoxy	is in range	40	70	1	1	3

3. Results and Discussion

3.1 Physical Observation

The physical observations of the produced composite samples (Fig.3.0) reveal distinctive characteristics in terms of smoothness, hardness, weight, and color. The physical observations provide valuable insights into the surface characteristics, hardness, weight, and color uniformity of the produced composite samples.

Smoothness: The analysis indicates that samples (Fig. 3.0) with a higher proportion of RHK and BFS exhibit a smoother surface compared to those with a lower composition of these components. Conversely, samples with a higher concentration of epoxy resin tend to have rougher surfaces. This observation suggests a correlation between the composition of the materials and the resulting surface texture.

Hardness: The findings highlight that samples (Fig. 3.0) with a predominant composition of BFS demonstrate enhanced hardness when compared to those with a higher proportion RHK or a combination of both RHK and BFS. This insight into hardness variations provides valuable information on the structural integrity and strength of the composite materials.

Weight: The weight observation reveals a trend where samples with a higher content of RHK, BFS, or a combination of both tend to weigh more than those with a higher concentration of epoxy resin. This disparity in weight is attributed to the density and composition of the materials used, shedding light on the overall mass characteristics of the produced composite samples.

Color: The color analysis indicates a uniform blue hue across all samples, attributed to the color of the epoxy resin employed in the manufacturing process. This consistent coloration ensures that the visual aspect of the samples remains constant, allowing for standardized evaluation.

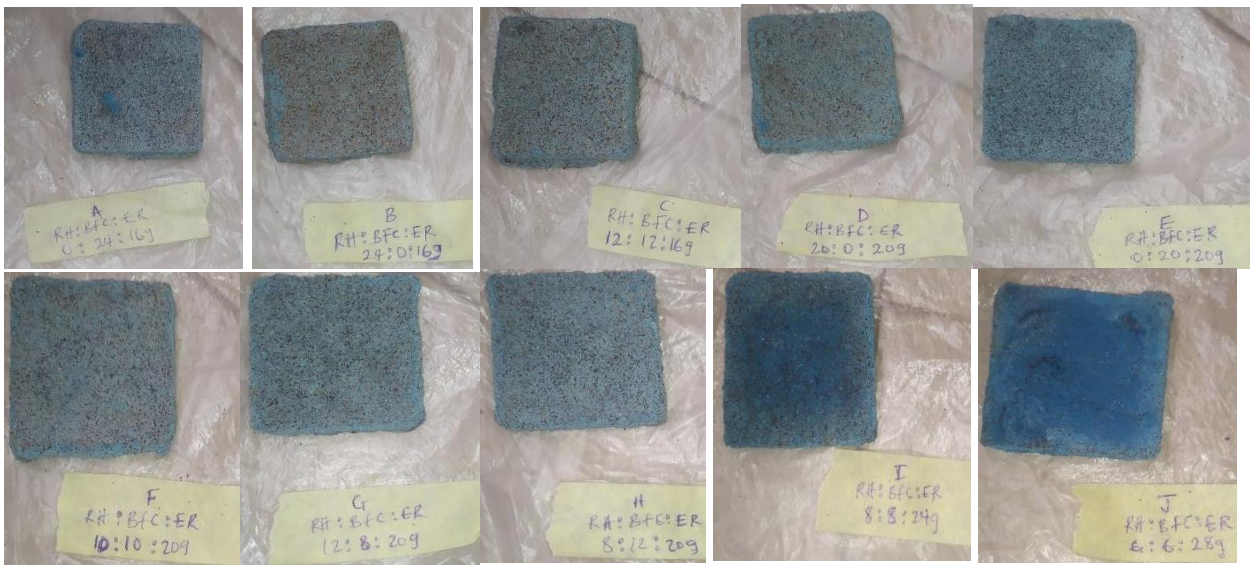

Fig. 3 Samples of fiberboard produced

3.2. Density of the Composite

The analysis of composite densities in this study, as presented in Table 2, provides valuable insights into the material properties and their implications for various applications. Among the samples (A-J), Sample D, with a percentage composition of 50:0:50 of RHK:BFS:EPR, recorded the highest density of 7.04 g/cm³. Following closely, Sample C, with a composition of 30:30:40, exhibited a density of 6.55 g/cm³. These findings underscore the influence of varying compositions on the resulting densities, offering valuable considerations for tailored material properties. The observed density range across all samples, from 7.04 to 5.81 g/cm³, signifies a relatively narrow distribution. Despite the diverse percentage compositions used, the samples exhibit comparable densities within this range. Notably, Samples D, C, B, J, A, E, and I were characterized by relatively low densities, indicating that the composite materials produced are lightweight. This characteristic is significant as it suggests that the composites maintain favorable qualities associated with lightweight materials while also offering versatility in composition. Sample F emerges as the lightest composite, boasting a density of 5.81 g/cm³. This sample has a percentage composition of 25:25:50 of RHK:BFS:EPR, signifying an equal volume distribution of rice husk and breadfruit coat. This specific composition yields a composite with reduced density, emphasizing the potential application in scenarios where lightweight materials are

crucial. Notably, this combination is highlighted as beneficial for the production of fiber, as it imparts a lightweight characteristic to the composite. In recent literature, similar trends and considerations in composite density optimization have been explored by various researchers **[6]**. The detailed analysis of composite densities in this study aligns with the broader trends observed in recent literature. The consideration of varying compositions and their effects on density is a common thread in the pursuit of lightweight yet durable composite materials, highlighting the versatility and potential applications of these materials in various industries

Table 2: Density of composite samples.

samples	Percentage Composition RHK:BFS:EPR (%)	Weight Composition RHK:BFS:EPR (g)	Mass(g)	Volume(cm^3)	Density(g/cm^3)
A	0:60:40	0:24:16	115.65	18.07	6.40
B	60:0:40	24:0:16	126.20	19.36	6.52
C	30:30:40	12:12:16	125.35	19.15	6.55
D	50:0:50	20:0:20	117.45	16.69	7.04
E	0:50:50	0:20:20	98.50	15.49	6.36
F	25:25:50	10:10:20	99.45	17.11	5.81
G	30:20:50	12:8:20	99.15	16.51	6.01
H	20:30:50	8:12:20	100.90	16.66	6.06
I	20:20:60	8:8:24	92.15	15.14	6.09
J	15:15:70	6:6:28	83.10	12.95	6.41

3.3. Water Absorption Capacities of the Sample

The assessment of water absorption capacities in samples A-J, as presented in Table 3 provides crucial insights into the materials' ability to resist water penetration. The results reveal notable variations in absorption capacities, with implications for the potential applications of these composite materials. Sample A exhibited the highest water absorption capacity at 19.93%, indicating a relatively higher susceptibility to water penetration. Following closely, samples C and B recorded absorption capacities of 17.63% and 16.24%, respectively. These results suggest that the percentage composition of rice husk (RHK), breadfruit coat (BFS), and epoxy resin (EPR) plays a significant role in determining the water absorption characteristics of the composites. Samples E, H, and D displayed the next highest absorption capacities, with values of 14.52%, 14.37%, and 13.96%, respectively. These compositions demonstrate a moderate resistance to water absorption, reflecting a balanced combination of the waste materials and epoxy resin. Conversely, samples G, F, I, and J exhibited lower water absorption capacities, ranging from 13.76% to 5.42%. Notably, sample J, with a composition of 15:15:70 of RHK:BFS:EPR, displayed the least water absorption capacity. This composition, characterized by a higher percentage of epoxy resin, aligns with the expectation that a composite with more binder content tends to have lower water absorption. This characteristic is particularly advantageous as low water absorption is desirable for composite materials, enhancing their durability and longevity. Sample I, with a composition of 20:20:60, also demonstrated lower water absorption capacities (10.96%) compared to other compositions. This observation further supports the trend that compositions with lower epoxy resin content exhibit higher absorption capacities, emphasizing the role of binder content in influencing water absorption. The correlation between epoxy resin content and water absorption capacities is highlighted in the findings. Compositions with lower epoxy resin content tend to have higher absorption capacities [12], emphasizing the need for an adequate binder to protect the composite from water ingress. The water absorption results highlight the importance of composition in determining the water resistance of composite materials. The findings have implications for the optimization of composite formulations, guiding the development of materials with enhanced resistance to water penetration in various applications.

Table 3: Water absorption capacities of the samples

samples	Percentage Composition RHK:BFS:EPR (%)	Weight Composition RHK:BFS:EPR (g)	Initial mass(g)	DryWet mass(g)	Water Absorption rate (%)
A	0:60:40	0:24:16	115.65	138.70	19.93
B	60:0:40	24:0:16	126.20	146.70	16.24
C	30:30:40	12:12:16	125.35	147.45	17.63
D	50:0:50	20:0:20	117.45	133.85	13.96
E	0:50:50	0:20:20	98.50	112.80	14.52
F	25:25:50	10:10:20	99.45	112.95	13.57
G	30:20:50	12:8:20	99.15	112.80	13.76
H	20:30:50	8:12:20	100.90	115.20	14.37

I	20:20:60	8:8:24	82.15	102.25	10.96
J	15:15:70	6:6:28	83.10	87.60	5.42

3.4. Thickness Swelling Test

The results of the thickness swelling test, as presented in Table 4 offer insights into the dimensional stability of the composite samples. Thickness swelling is a critical parameter that influences the material's performance, especially in applications where dimensional stability is crucial. Sample A and I exhibited the highest thickness swelling values at 23.7% and 20.39%, respectively. These samples, with percentage compositions of 0:60:40 and 20:20:60 for RHK:BFS:EPR, suggest that variations in the composition significantly impact the swelling behavior. The higher values indicate a greater expansion in thickness, possibly due to a higher proportion of water absorption or other factors related to the specific compositions. Conversely, sample J and D demonstrated the lowest thickness swelling among the samples, recording values of 1.18% and 1.74%, respectively. The compositions for sample J and D were 50:0:50 and 15:15:70 for RHK:BFS:EPR. The lower thickness swelling in these samples implies enhanced dimensional stability, which is desirable for applications where changes in thickness can impact performance. The thickness swelling test results underline the sensitivity of composite dimensional stability to variations in composition. The findings align with trends observed in recent literature [13,14], emphasizing the need for careful consideration of material composition in the development of composites with optimal thickness swelling characteristics.

Table 4: Thickness swelling test

samples	Percentage Composition RHK:BFS:EPR (%)	Weight Composition RHK:BFS:EPR (g)	Initial Thickness (cm)	Final Thickness (cm)	Thickness Swell rate (%)
A	0:60:40	0:24:16	0.675	0.835	23.70
B	60:0:40	24:0:16	0.725	0.864	19.17
C	30:30:40	12:12:16	0.718	0.841	17.13
D	50:0:50	20:0:20	0.748	0.761	1.74
E	0:50:50	0:20:20	0.602	0.690	14.61
F	25:25:50	10:10:20	0.609	0.695	14.12
G	30:20:50	12:8:20	0.599	0.694	15.86
H	20:30:50	8:12:20	0.652	0.706	8.28
I	20:20:60	8:8:24	0.505	0.608	20.39
J	15:15:70	6:6:28	0.592	0.599	1.18

3.5. Optimization Results

To explore the combined impact of independent variables, Box-Benkhen Design (BBD) was employed across 8 experimental sets. This approach bypasses the time-consuming phase inherent in one-factor-at-a-time methods [15,16,17]. BBD's proficiency in fitting quadratic surfaces makes it particularly suitable for process optimization while minimizing the required number of experiments [18,19]. Experimental data on % Thickness Swell, Water Absorption (%), and Density (kg/cm^3) under various conditions for fiberboard production are presented in Tables 5 and plotted in Fig.4.0. Optimization was performed using Design Expert Version 10.0.1.

Table 5 CCD matrix of the response variables

Run	A:RHK(g)	B:BFS(g)	C:EPR(g)	Thickness Swelling(%)	Water Absorption(%)	Density(g/cm3)
1	20	40	10	49.3333	19.9609	7.98287
2	20	0	15	15.9091	19.8967	6.73142
3	0	20	15	11	51.403	6.61822
4	20	0	10	9.1	21.256	6.11622
5	0	40	12.5	39	26.9176	7.4047
6	15	10	12.5	5.7971	27.9807	5.98464
7	20	20	12.5	21.2121	30.511	6.05223
8	20	20	12.5	14.2857	32.5686	5.93299
9	20	20	12.5	15.5556	30.0815	5.8681
10	40	20	10	11	28.8992	6.40433

11	20	20	12.5	5	38.8635	6.15003
12	40	0	12.5	4.21053	5.8899	6.00274
13	20	40	15	15.5844	26.4584	6.19081
14	40	20	15	13.3333	17.0854	5.97681
15	0	20	10	36.1905	31.5556	7.44922
16	40	40	12.5	6.52174	3.8239	6.24986
17	20	20	12.5	11.9048	18.3235	5.8258

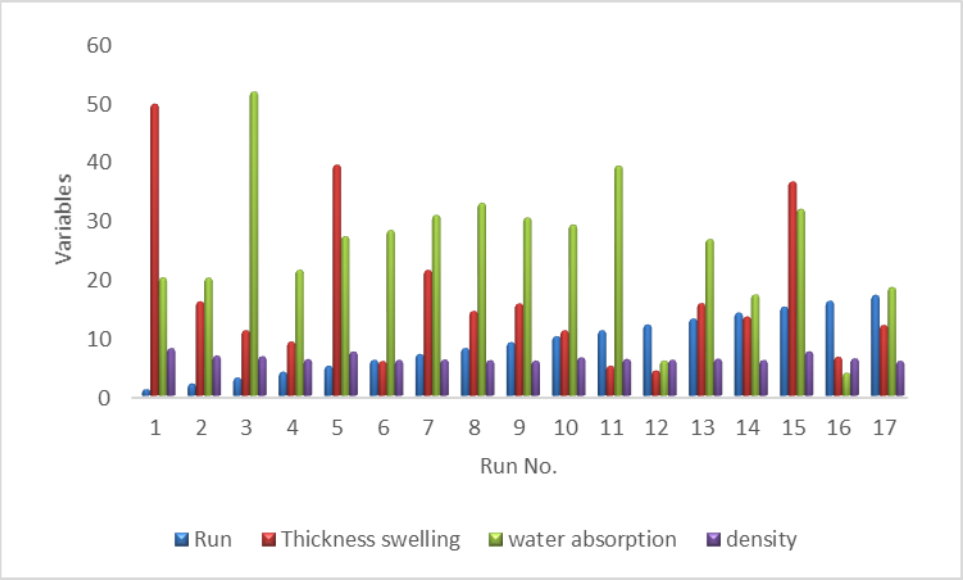

Fig. 4: Response variables in the Fiberboard production

3.6. Statistical analysis

The evaluation of the regression model's validity employed Analysis of Variance (ANOVA), incorporating various descriptive statistics such as probability value (p-value), F-value, coefficient of determination (R^2), adjusted coefficients of determination (adj R^2), and degrees of freedom (df). The ANOVA summary of the responses: Thickness swelling test, water absorption test and density of sample are presented in Tables 6-8. The F-value compared curvature variance with residual variance, while the p-value indicated the probability of obtaining the observed F-value under the null hypothesis. A confidence level of 95% ($\alpha = 0.05$) governed the determination of statistical significance. A small p-value ($p < 0.05$), as noted by Abonyi et al. [17], signaled a highly significant model conducive to accurate prediction [20]. The model's goodness of fit relied on the determination coefficient (R^2) [21,22], with a value of 0.9427, 0.8918 and 0.9883 for thickness swelling test, water absorption and density of sample, respectively. This indicate a high degree of correlation between observed and predicted values. This suggested that 94.27, 89.18 and 98.83% of the variability in the fiberboard production process was explained by the independent variables. Adequate precision, assessed through a value exceeding 4 [23], affirmed the model's efficacy, with a value of 12.495, 10.91 and 25.345 for thickness swelling test, water absorption and density of sample, respectively, indicating adequacy of the model developed. Moreover, the small value of standard deviation: 4.65, 5.64 and 0.1 for thickness swelling test, water absorption and density of sample, respectively, compared to the mean confirmed the selected quadratic model's suitability for correlating experimental data (Tables 6-8). The descriptive statistics collectively highlighted the high significance, adequacy, accurate predictability, and reasonable reproducibility of the selected second-order polynomial regression model adequacy, accurate predictability, and reasonable reproducibility of the selected second-order polynomial regression model.

Table 6: ANOVA table for thickness swelling test

Source	**Squares**	**df**	**Square**	**Value**	**Prob > F**	
Model	2492.44	9	276.94	12.81	0.0014	significant
A-RHK	194.05	1	194.05	8.97	0.0201	
B-BFS	673.39	1	673.39	31.14	0.0008	
C-EPR	309.97	1	309.97	14.33	0.0068	
AB	218.26	1	218.26	10.09	0.0156	
AC	189.39	1	189.39	8.76	0.0211	

BC	411.24	1	411.24	19.02	0.0033	
A^2	32.35	1	32.35	1.50	0.2609	
B^2	6.32	1	6.32	0.29	0.6055	
C^2	225.93	1	225.93	10.45	0.0144	
Residual	151.39	7	21.63			
Lack of Fit	12.31	3	4.10	0.12	0.9448	not significant
Pure Error	139.07	4	34.77			
Cor Total	2643.82	16				

Std. Dev.	4.65	R-Squared	0.9427
Mean	16.76	Adj R-Squared	0.8691
C.V. %	27.75	Pred R-Squared	0.6859
PRESS	830.48	Adeq Precision	12.495

Table 7: ANOVA table for water absorption test

Source	**Squares**	**df**	**Square**	**Value**	**Prob > F**	
Model	1836.69	9	204.08	6.41	0.0114	significant
A-RHK	479.87	1	479.87	15.08	0.0060	
B-BFS	9.91	1	9.91	0.31	0.5943	
C-EPR	21.69	1	21.69	0.68	0.4363	
AB	11.48	1	11.48	0.36	0.5671	
AC	250.61	1	250.61	7.87	0.0263	
BC	15.43	1	15.43	0.48	0.5087	
A^2	26.60	1	26.60	0.84	0.3910	
B^2	580.36	1	580.36	18.23	0.0037	
C^2	91.01	1	91.01	2.86	0.1347	
Residual	222.79	7	31.83			
Lack of Fit	1.05	3	0.35	6.315E-003	0.9992	not significant
Pure Error	221.74	4	55.44			
Cor Total	2059.49	16				

Std. Dev.	5.64	R-Squared	0.8918
Mean	25.38	Adj R-Squared	0.7527
C.V. %	22.23	Pred R-Squared	0.8279
PRESS	354.39	Adeq Precision	10.910

Table 8: ANOVA table for Density of the sample

Source	**Squares**	**df**	**Square**	**Value**	**Prob > F**	
Model	6.37	9	0.71	65.87	< 0.0001	significant
A-RHK	0.94	1	0.94	87.41	< 0.0001	
B-BFS	0.59	1	0.59	55.14	0.0001	
C-EPR	0.74	1	0.74	69.03	< 0.0001	
AB	0.070	1	0.070	6.56	0.0375	
AC	0.041	1	0.041	3.79	0.0926	
BC	1.45	1	1.45	134.88	< 0.0001	

A^2	0.14	1	0.14	13.22	0.0083	
sB^2	0.41	1	0.41	38.08	0.0005	
C^2	0.71	1	0.71	65.96	< 0.0001	
Residual	0.075	7	0.011			
Lack of Fit	3.551E-003	3	1.184E-003	0.066	0.9751	not significant
Pure Error	0.072	4	0.018			
Cor Total	6.44	16				

Std. Dev.	0.10	R-Squared	0.9883
Mean	6.41	Adj R-Squared	0.9733
C.V. %	1.62	Pred R-Squared	0.9717
PRESS	0.18	Adeq Precision	25.345

The empirical relationship linking the percentage thickness swelling test, percentage water absorption and density of the sample to the process variables: quantity of BFS, quantity of RHK and quantity of EPR was derived using Design Expert 10.0.1 and is expressed in Equations 1-3. Here, A, B and C represent the coded values corresponding to the quantity of BFS, quantity of RHK, and quantity of EPR, respectively.

Y_1 = 13.19-5.87A+10.75B-6.22C-10.14AB+6.88AC-10.14BC-3.2A^2+1.37^2+7.86C^2 (1)
Y_2 = 30.07-9.23A+1.3B+1.65C-2.32AB-7.92AC+1.96BC-2.82A^2-13.17B^2+4.99C^2 (2)
Y_3 = 5.97-0.41A+0.32B-0.3C-0.18AB+0.1AC-0.6BC+0.35B^2+0.44C^2 (3)

Coefficients involving single factors represent the impact of those specific factors, while coefficients involving multiple factors denote interactions between those factors. A positive coefficient signifies a synergistic effect, whereas a negative coefficient indicates an antagonistic effect of the factor. A model is deemed significant if the p-value is below 0.05 [17]. From the presented p-values in Table 6, it is evident that the linear terms A, B, and C, the interaction terms AB, AC, BC and the quadratic terms C^2 are significant model components. Table 7 also showed that the only significant term for water absorption test were AC and B^2. According to Table 8, for density of sample, the significant terms remaining after the insignificant terms were remove were A, B, C, AB,, BC, B^2 and C^2. Insignificant terms were omitted, leading to the reduction of the model to Eq. 4-6

Y_1 = 13.19-5.87A+10.75B-6.22C-10.14AB+6.88AC-10.14BC+7.86C^2 (4)
Y_2 = 30.07-7.92AC-13.17B^2 (5)
Y_3 = 5.97-0.41A+0.32B-0.3C-0.18AB-0.6BC+0.35B^2+0.44C^2 (6)
Where $Y_1, Y_2 and\ Y_3$ represent the model equation for thickness swelling test, water absorption and density of the samples.

3.7 Response Surface Results

The 3D response surface plots illustrating the combined effects of water-based breadfruit seed filler (BFS), rice husk (RHK), and epoxy resin (EPR) on water absorption (%), density (kg/cm³), and thickness swell (%) for fiberboard production are depicted in Figures 5a through 7c. These response surfaces were generated by varying two factors while holding the third constant. Figures 5a and 7a demonstrate that an increase in the rice husk/breadfruit filler ratio leads to higher Thickness and density of the sample, whereas increasing the epoxy resin ratio results in decreased water absorption. Similarly, Figure 6a. reveals that increase in the rice husk/breadfruit filler ratio reduces the water absorption capacity, while increasing the epoxy resin ratio decreases water absorption (Fig. 6c). Likewise, Figure 7b illustrates that increasing the rice husk ratio increases density, while increasing the epoxy resin ratio decreases density. Optimization investigations become essential when the collective impact of independent factors significantly influences the overall response or output [24,25,26]. Utilizing the optimization tool yielded an optimal composition of 14.667 g RHK, 38.665 g BFS, and 12.653 g EPR, resulting in a ceiling board with a density of 6.001g/cm³, thickness swell of 9.81%, and water absorption of 4.016%.
A water absorption rate as low as 4.016% is advantageous for a ceiling board, particularly in scenarios involving a leaking roof sheet. Additionally, a low thickness swell indicates minimal deformation of the ceiling board when exposed to moisture.

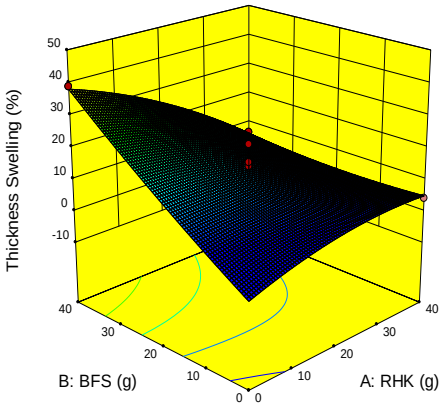

Fig. 5a: 3D plot of BFS and RHK for thickness

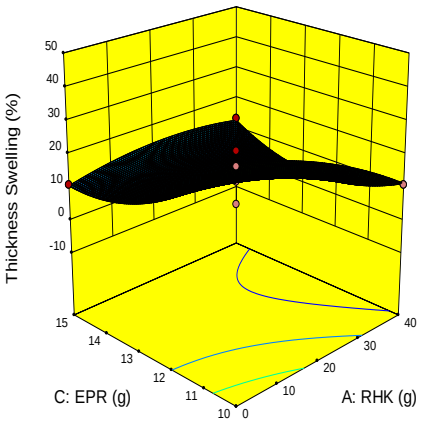

Fig. 5b: 3D plot of EPR and RHK for thickness

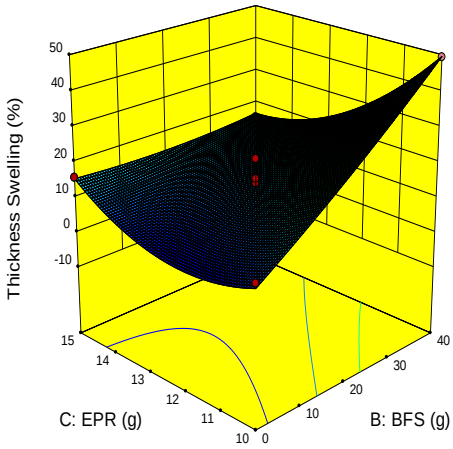

Fig. 5c: 3D plot of EPR and BFS for thickness

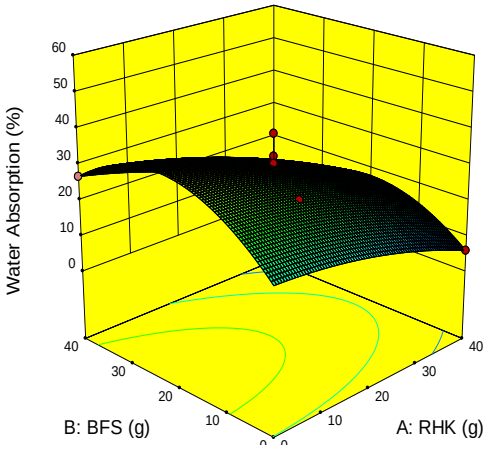

Fig. 6a: 3D plot of BFS and RHK for water absorption

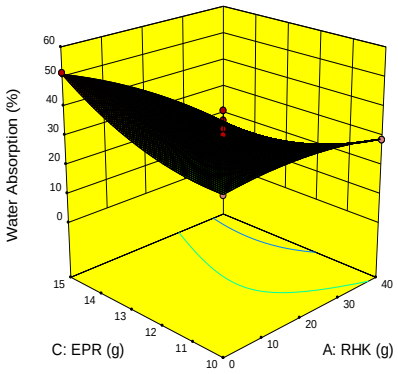

Fig. 6b: 3D plot of EPR and RHK for water absorption

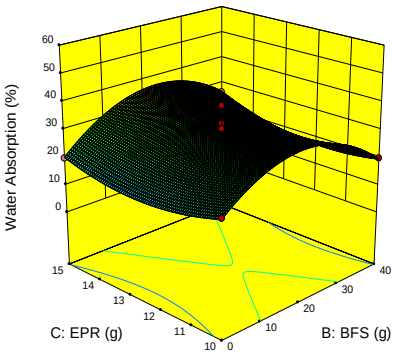

Fig. 6c: 3D plot of EPR and BFS for water absorption

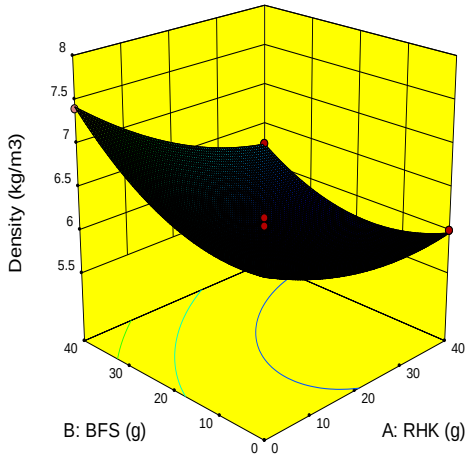

Fig. 7a: 3D plot of BFS and RHK for Density of sample

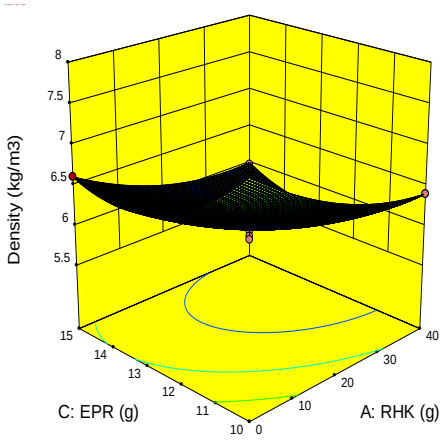

Fig. 7b: 3D plot of EPR and RHK for Density of sample

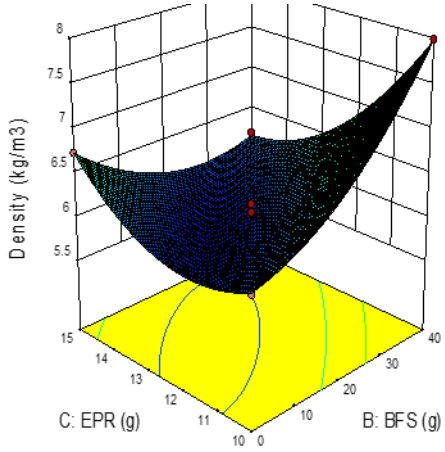

Fig. 7C: 3D plot of EPR and BFS for Density of sample

4. Conclusion

The incorporation of Breadfruit Seed (BFS) and Rice Husk (RHK) fibers as sustainable reinforcements for Epoxy Resin (EPR) matrices presents promising outcomes. The resulting composite materials demonstrate a narrow density range (5.81-7.04 g/cm³), which showed their lightweight nature, a critical attribute for diverse applications. Variations in water absorption capacities, influenced by composition, highlight the higher absorption rates associated with lower epoxy resin content, while thickness swelling results showed the importance of thorough material formulation for optimal dimensional stability. These findings harmonize with recent literature trends, emphasizing the essential role of composition in attaining desired properties. Moreover, the study's comprehensive methodology and outcomes provide valuable insights into the potential of BFS and RHK as eco-friendly reinforcements. They pave the way for the development of sustainable composite materials with diversified applications and enhanced performance. Furthermore, Utilizing the optimization tool yielded an optimal composition of 14.667 g RHK, 38.665 g BFS, and 12.653 g EPR, resulting in a ceiling board with a density of 6.001g/cm³, thickness swell of 9.81%, and water absorption of 4.016%.

Acknowledgement

This research was funded by Tertiary Education Trustfund, Nigeria through institution based research intervention.

References

[1] Duke AE, Eno EE. Utilization of Rice Husk Ash as a Partial Replacement for Cement in Concrete Production. Journal of Sustainable Development. 2019; 12(3): 123-137.

[2] Amit A, Ipshita I. A Review on Agricultural Waste Utilization as a Sustainable Building Material. International Journal of Sustainable Built Environment. 2015; 4(2): 197-217.

[3] Olorunmaiye KS, Ohijeagbon O. Feasibility of Using Jatropha Curcas Seedcake as a Raw Material for Ceiling Board Production. Journal of Renewable Materials. 2015; 3(4): 343-356.

[4] Idris UD, Aigbodion VS, Atuanya CU. Eco-friendly (water melon peels): alternatives to wood-based particleboard composites. Tribology in industry. 2011:33(4): 173.

[5] Chibudike HO, Anyakora AN, Suleiman M A, Adeyoju OA, Aruwolo AB, Akabeze EU, Samuel AE. Utilization of baamboo in the production of ceiling board. J. Eng. Res. 2011; 16(1): 1-10.

[6] Amenaghawon NA, Osayuki-Aguebor W, Okieimen CO. Production of particle boards from corn cobs and cassava stalks: Optimization of mechanical properties using response surface methodology. J. Mater. Environ. Sci. 2016; 7(4): 1236-1244.

[7] Ang PSE, Ibrahim AHI, Abdullah MS. Preliminary study of ceiling board from composite material of rice husk, rice husk ash and waste paper. Progress in Engineering Application and Technology. 2020; 1(1): 104-115.

[8] Eric G K, Hensley B K; Analysis of the Thermal Insulation Properties of Rice Husk Ceiling Board Compared to Selected Fibre Based Ceiling Materials Used in Yola Metropolis, Adamawa State Nigeria. American Journal of Mechanical and Materials Engineering. 2019; 1(4): 83-88.

[9] Neku MN. Evaluation of properties of laterite-rice husk fibre ceiling tiles produced with locust bean pod solution as binder (doctoral dissertation). 2023.

[10] Zeleke Y, Rotich GK. Design and development of false ceiling board using polyvinyl acetate (PVAc) composite reinforced with false banana fibres and filled with sawdust. International Journal of Polymer Science. 2021;1-10.

[11] Ezenwa ON, Obika EN, Umembamalu CJ, Nwoye. Development of ceiling board using breadfruit seed coat and recycled low density polyethylene. Heliyon. 2019; 5(11).

[12] Akinyemi BA, Okonkwo CE, Alhassan EA, Ajiboye M. Durability and strength properties of particle boards from polystyrene–wood wastes. Journal of Material Cycles and Waste Management. 2019; 21: 1541-1549.

[13] Medved S, Tudor EM, Barbu MC, Jambrekovic V, Španic N. Effect of Pine (Pinus Sylvestris) Bark Dust on Particleboard Thickness Swelling and Internal Bond. Drv. Ind. 2019; 70: 141-147.

[14] López YM, Paes JB, Rodríguez EM, Gustave D, Gonçalves FG. Wood particleboards reinforced with thermoplastics to improve thickness swelling and mechanical properties. Cerne. 2018; 24: 369-378.

[15] Nwadike EC, Abonyi MN, Onu CE, Obika EN. Synthesis and optimization of biodiesel from soybean. International journal of mechanical and production engineering (IJMPE). 2019; 7(12); 2321-2071.

[16] Nwadike EC, Abonyi MN, Nwabanne JT, Ohale PE. Optimization of Solar Drying of Blanched and Unblanched Aerial Yam using Response Surface Methodology" International Journal of Trend in Scientific Research and Development (ijtsrd). 2020; 4(3).

[17] Abonyi MN, Aniagor CO, Menkiti MC. Statistical Modelling Of The Adsorptive Dephenolation of Petroleum Industry Wastewater using Ionic Liquid Treated Clay. Sigma: Journal of Engineering & Natural Sciences/Mühendislik Ve Fen Bilimleri Dergisi. 2020; 38(3).

[18] Kumar V, Kharub M, Sinha A. Modeling and optimization of turning parameters during machining of AA6061 composite using RSM box-behnken design. In IOP Conference Series: Materials Science and Engineering. 2021; 1057(012058). IOP Publishing.

[19] Mathivanan K, Thirumalaikumarasamy D, Ashokkumar M, Deepak S, Mathanbabu M. Optimization and prediction of AZ91D stellite-6 coated magnesium alloy using Box Behnken design and hybrid deep belief network. journal of materials research and technology. 2021; 15: 2953-2969.

[20] Kumari N, Arya S, Behera M, Seth C S, Singh R. Chitosan anchored nZVI bionanocomposites for treatment of textile wastewater: Optimization, mechanism, and phytotoxic assessment. Environmental Research. 2024; 245: 118041.

[21] Varol Özkavak H, Ince M, Bıçaklı EE. Prediction of mechanical properties of the 2024 aluminum alloy by using machine learning methods. Arabian Journal for Science and Engineering. 2023; 48(3): 2841-2850.

[22] Ahmad SA, Rafiq SK Numerical modeling to predict the impact of granular glass replacement on mechanical properties of mortar. Asian Journal of Civil Engineering. 2024; 25(1); 19-37.

[23] Chary PS, Bansode A, Rajana N, Bhavana V, Singothu S, Sharma A, Mehra NK. Enhancing breast cancer treatment: Comprehensive study of gefitinib-loaded poloxamer 407/TPGS mixed micelles through design, development, in-silico modelling, In-Vitro testing, and Ex-Vivo characterization. International Journal of Pharmaceutics. 2024; 124109.

[24] Ohale PE, Chukwudi K, Ndive JN, Madiebo EM, Abonyi MN, Chukwu MM , Obi CC, Onu CE, Igwegbe CA, Azie CA. Optimization of Fe2O3@BC-KC composite preparation for adsorption of Alizarin red S dye: Characterization, kinetics, equilibrium, and thermodynamic studies, Results in Surfaces and interfaces, xxx(xxxx). 2023; 100157.

[25] Abonyi MN, Nwabanne JT, Ohale PE, Nwadike EC, Igbonekwu LI, Chukwu MM, Madiebo EM. Application of RSM and ANFIS in the optima parameter evaluation for crude oil degradation in contaminated water amended with PES, Case Studies in Chemical and Environmental Engineering. 2023; 8: 100483.

[26] Ohale PE, Ejimofor MI, Onu CE, Abonyi MN, Ohale JN. Development of a surrogate model for the simulation of anaerobic co-digestion of pineapple peel waste and slaughterhouse wastewater: Appraisal of experimental and kinetic modeling, Environmental Advances. 2023;11: 100340. https://doi.org/10.1016/j.envadv.2022.100340